
Molecular Crystals and Liquid Crystals

Publication details, including instructions for authors and subscription information:
http://www.tandfonline.com/loi/gmcl20

# Regular Defect Array Formed after Shear in Water-in-Cholesteric Liquid Crystal Emulsions

Makoto Yada [a], Jun Yamamoto [a] & Hiroshi Yokoyama [b]

[a] Yokoyama Nano-structured Liquid Crystal Project, ERATO, JST, Ibaraki, Tsukuba, Japan

[b] Yokoyama Nano-structured Liquid Crystal Project, ERATO, JST, Nanotechnology Research Institute, Ibaraki, Tsukuba, Japan

Version of record first published: 18 Oct 2010

To cite this article: Makoto Yada, Jun Yamamoto & Hiroshi Yokoyama (2004): Regular Defect Array Formed after Shear in Water-in-Cholesteric Liquid Crystal Emulsions, Molecular Crystals and Liquid Crystals, 409:1, 119-123

To link to this article: http://dx.doi.org/10.1080/15421400490435855

*Mol. Cryst. Liq. Cryst.*, Vol. 409, pp. 119–125, 2004

ISSN: 1542-1406 print/1563-5287 online
DOI: 10.1080/15421400490435855



# REGULAR DEFECT ARRAY FORMED AFTER SHEAR IN WATER-IN-CHOLESTERIC LIQUID CRYSTAL EMULSIONS

*Makoto Yada, Jun Yamamoto*
*Yokoyama Nano-structured Liquid Crystal Project, ERATO, JST, 5-9-9, Tokodai, Tsukuba, Ibaraki, 300-2635, Japan*

*Hiroshi Yokoyama*
*Yokoyama Nano-structured Liquid Crystal Project, ERATO, JST, 5-9-9, Tokodai, Tsukuba, Ibaraki, 300-2635, Japan and Nanotechnology Research Institute, National Institute of Advanced Industrial Science and Technology, 1-1-1 Umezono, Tsukuba, Ibaraki, 305-8568, Japan*

*We have investigated the spontaneous formation of the regular quadrilateral defect array in cholesteric emulsions, composed of water, surfactants, and cholesteric liquid crystals. Both at the substrate surface and at the surfactant-coated droplet surface, a homeotropic anchoring is enforced to the adjacent liquid crystal. We observe nucleation of numerous point defects, in the cholesteric planar texture immediately after termination of shear to the emulsion, which leads to the formation of the regular defect array. Two distinct steps were identified in the formation process; the first step is the nucleation and growth process of point defects, and the second step is the rearrangement process of point defects to the regular defect array.*

*Keywords*: anchoring; cholesteric; emulsion; nucleation; point defect

## INTRODUCTION

In liquid crystal emulsions, which are the system of water droplets dispersed in a liquid crystal host [1], a water droplet distorts the orientation of the adjacent liquid crystal, when the surface anchoring is sufficiently large. The induced elastic distortion extends over a long distance in liquid crystals, and creates novel interactions between water droplets [2].

Address correspondence to Makoto Yada, Yokoyama Nano-Structured Liquid Crystal Project ERATO, JST 5-9-9 Tokodai, Tsukuba, Ibaraki 300-2635 Japan.

Recently, liquid crystal emulsions have attracted considerable interest, particularly nematic emulsions [1–6] and microemulsions [7]. Here, we focus on cholesteric emulsions, composed of water, surfactants and cholesteric liquid crystals, whose phase has a spontaneous long-range helical structure, although its local molecular ordering is identical to that of a nematic phase. We have found the spontaneous formation of the regular quadrilateral defect array after applying the shear in the cholesteric emulsions. We will discuss the formation mechanism of the regular quadrilateral defect array, from the results of the microscopic observation and two-dimensional fast Fourier transform (2D FFT) image analysis in the cholesteric emulsions.

## EXPERIMENTAL SECTION

Two kinds of chiral nematic liquid crystals with different pitch ($p \sim 0.33$ and 11.1 μm) were used in this study. The 0.33 μm-pitch cholesteric is a mixture of base nematics shown in Figure 1 (Cr 11 °C N 116°C I, from Dainippon ink & Chemicals) and a chiral dopant CB-15 (40 wt%, from Merck). The isotropic-cholesteric phase-transition temperature ($T_{Iso\text{-}Ch}$) has been identified to be 49°C, examined by microscopic observation. On the other hand, the 11.1 μm-pitch cholesteric is composed of base nematics (ZLI-1132, from Merck) and CB-15 (1 wt%), with $T_{Iso\text{-}Ch} \sim 74$°C.

Water-in-cholesteric liquid crystal emulsions were prepared by mixing 90 wt% didodecyl dimethyl ammonium bromide (DDAB) aqueous solution into cholesteric liquid crystals in the isotropic phase. DDAB was used to stabilize small water droplets in cholesteric liquid crystals. The weight concentration of the DDAB aqueous solution in the emulsion, $C_w$, was changed between 0.5 and 2 wt%. The isotropic-cholesteric phase transition temperature became at most 2°C lower than that of the corresponding pure cholesteric liquid crystals. When the liquid crystal is in the isotropic phase, this system is equivalent to conventional water-in-oil microemulsions.

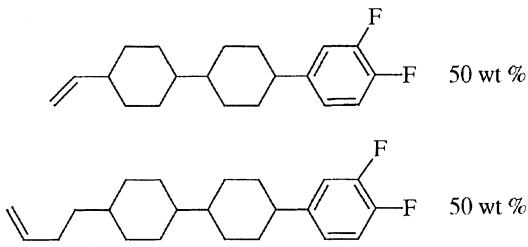


**FIGURE 1** Chemical structure of one of base nematic mixtures.

When temperature goes down to the cholesteric phase, water droplets appear by macroscopic phase separation. (We confirmed directly the appearance of micron-size water droplets in parallel plate cells with a homogeneous anchoring condition.) The anchoring at the droplet surface is likely to be homeotropic due to the adsorption of surfactant molecules.

Textures of the cholesteric emulsions were observed under a polarizing microscope at 30°C. Samples were sandwiched between a pair of glass plates with homeotropic anchoring, and the thickness was controlled from 10 to 100 μm. The cholesteric emulsion sample was subjected to a fairly strong shear of 500–1000 $s^{-1}$ on a hot stage.

2D FFT image analysis was performed to observed textures by using the software of Image-Pro Plus ver.4 (from Media Cybernetics). In case of the direct application of 2D FFT to polarizing microscope images, the information of the anisotropy is included in FFT spectrum. To avoid the influence of the birefringent contrast, we first generated a mesh, whose segment was so drawn as to connect nearest neighbor point defects. These connecting lines carry all necessary information about the periodicity and the orientation of the defect array.

## RESULTS AND DISCUSSIONS

In general, pure cholesteric liquid crystals show a planar texture, i.e. the Grandjean texture under a sufficiently large shear. This is because liquid crystal molecules tend to realign along the flow to minimize the viscous dissipation. The Grandjean texture induced by the shear remains stable even in homeotropically aligning cells, as long as the cholesteric pitch is much smaller than the sample thickness and/or the temperature is far away from the cholesteric to isotropic transition. On the contrary, the shear-induced Grandjean texture in cholesteric emulsions cannot be stable in a homeotropic cell for any pitch length and at any temperature. Figure 2(a)–(b) show the distortion of the Grandjean texture induced after the shear to the cholesteric emulsion comprised of water droplets ($C_w = 2\,wt\%$) and the cholesteric ($p = 0.33\,\mu m$). The sample thickness is fixed at 10 μm. Immediately after stopping the shear, numerous point defects are created in the planar texture as shown in Figure 2(a). The size of the single defect grows, while undergoing rapid coalescence with neighboring defects, and the point defects tend to assume a regular arrangement, which leads to the regular defect array shown in Figure 2(b). Figure 3 shows the time dependence of the density and the size of point defects after stopping the shear. In the early stage until $t \sim 10\,s$, the density and the size of point defects steeply increase, and the defects fill up all the available space around $t = 10\,s$. In the following late stage, the density gradually decreases with

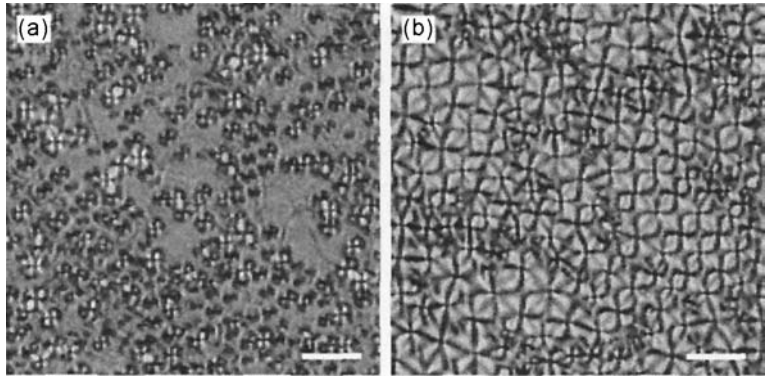


**FIGURE 2** Formation of the regular defect array after stopping the shear in the cholesteric emulsion ($C_w = 2.0\,wt\%$, $p = 0.33\,\mu m$). (a) $t = 3\,s$ after stopping the shear, (b) $t = 1\,min$. The sample thickness is $10\,\mu m$. Scale bar; $20\,\mu m$. (Under cross polarizers.)

time, whereas the size increases. In this stage, the defect size and the defect density are no longer independent as in the early stage, because the point defects are already virtually close packed. After $t > 100\,s$, the density and the size of point defects tend to be constant, which means the construction of the stabilized defect array. The growth rate of the density and the

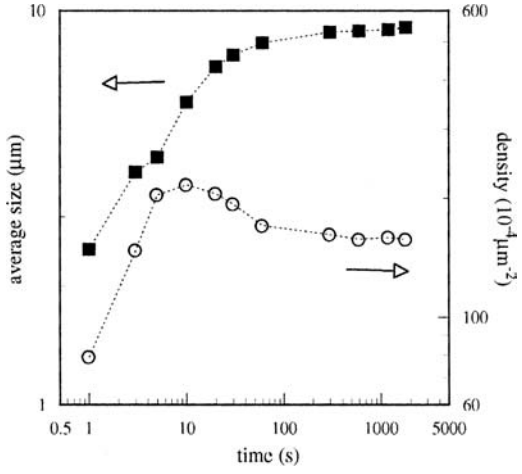


**FIGURE 3** Time dependence of the density and the size of point defects after stopping the shear ($C_w = 2.0\,wt\%$, $p = 0.33\,\mu m$). The size of point defects is defined as their average radius. The sample thickness is $10\,\mu m$.

size in the early stage and the equilibrium period of the final defect array tend to be independent of the concentration of water droplets between 1 and 2 wt% (not shown in this paper). The formation of the defect array can be observed in temperature range from each isotropic-cholesteric phase transition temperature to room temperature (25°C) in both cholesterics with different pitch ($p \sim 0.33$ and 11.1 μm). On the other hand, the defect array can never be formed in samples sandwiched between homogeneous anchoring glass plates; here, water droplets readily coalesce after stopping the shear, eventually leaving only oily streaks in the planar texture.

For the long pitch cholesteric ($p = 11.1$ μm), the spatial distribution of cholesteric helix in the defect array is visually observable. As shown in Figure 4, the defect array is accompanied by a regular arrangement of concentric finger print patterns, which fills the entire volume between upper and lower glass surfaces. This result clearly shows that the defect array has a regular three-dimensional lattice of the cholesteric helix and point defects, presumably stabilized by the interplay between uniform helical order and homeotropic anchoring glass surfaces. This arrangement of the cholesteric helix closely resembles the cholesteric polygonal texture described by Bouligand [8] in early 1970's. The polygonal texture, however, was formed in certain neat cholesterics, and could appear only at a temperature close to the cholesteric–isotropic transition point. It should be noted that, in the absence of water droplets, the defect array can never be spontaneously generated well inside the cholesteric phase from the shear-induced planar-aligned samples.

To extract the information about the positional correlation among point defects, we carried out 2D FFT analysis. Figures 5(a)–(c) show the time evolution of the 2D FFT patterns for the case of 2.0 wt% DDAB aqueous

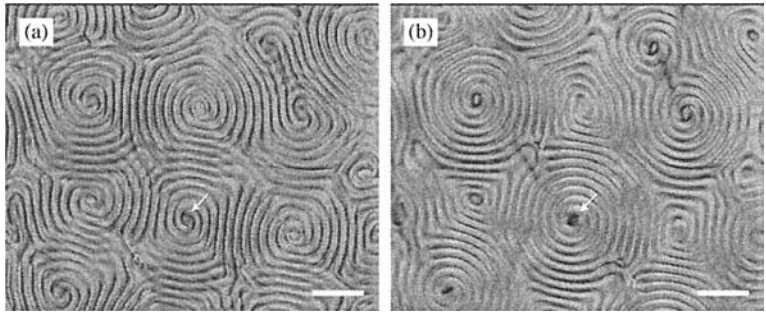


**FIGURE 4** Arranged concentric finger print texture in the defect array. (Cholesteric; ZLI-1132 + CB-15 (1 wt%). $C_w = 2.0$ wt%, $p = 11.1$ μm). The sample thickness is 50 μm. Scale bar: 50 μm. (a) Upper, and (b) lower surface. Arrows point at the same position.

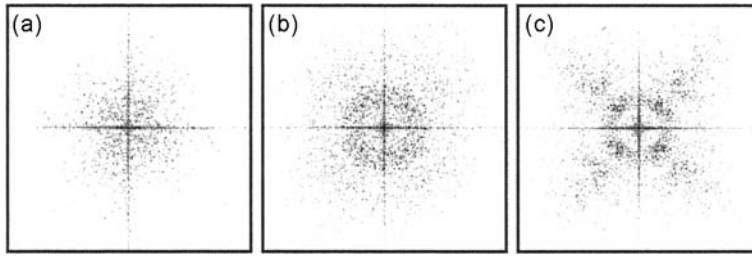


**FIGURE 5** 2D FFT patterns corresponding to the positional correlation of point defects. (a) $t = 3$s after stopping the shear, (b) $t = 10$ s, (c) $t = 1$ min ($C_w = 2.0$ wt%, $p = 0.33\,\mu$m).



solution, which provide us with the information on the periodicity and the orientational correlation of the defect array respectively. Immediately after stopping the shear ($t < 10$ s), only a highly diffuse scattering showed up, indicating the absence of any periodicity and orientational order among point defects, as shown in Figure 5(a). When all space was filled up by defects ($t \sim 10$ s), a scattering peak appeared as a ring shown in Figure 5(b), corresponding to the evolution of finite periodicity among point defects. This scattering ring became smaller with time, and at $t = 1$ min, it was split into four brush-like anisotropic scattering patterns, as shown in Figure 5(c). This result indicates the four-fold rotational symmetry of the defect array in consistent with the microscope image in Figure 2(b).

From the above results, we noticed two steps in the formation process of the defect array. The first step is the generation and growth of point defects from the shear-induced planar texture, and the second step is the rearrangement of the defects into the regular array after filling up all space of point defects. In the first step ($0 < t < 10$ s), there could in principle be two possible routes to the generation of point defects, i.e., nucleation-growth and spinodal decomposition [9,10]. A characteristic feature of a spinodal decomposition is that the wave number of the instability appears from its early stage. In our case, point defects are generated without any positional correlation as already confirmed in Figure 5(a). We have actually seen in Figure 2(a) that the size of point defects has a broad distribution in the first step, showing that the point defects were not simultaneously generated. This behavior is only consistent with the nucleation and growth mechanism.

Initially, the strong shear makes liquid crystal molecules aligned parallel to the glass plates, and makes water droplets fragmented and dispersed homogeneously at the same time. After removing the shear, the planar alignment begins to be distorted to restore homeotropic orientation induced by the anchoring effect on the glass plates. Since liquid crystalline

molecules must rearrange cooperatively in macroscopic length scales to transform the planar to the homeotropic orientation, the planar alignment never changes to the homeotropic in pure cholesterics without water droplets. Water droplets can strongly distort the orientation of the director owing to the homeotropic anchoring at the interface. Therefore, the shear-induced planar texture of cholesteric emulsions includes many defect cores and hence has a higher free energy than the pre-sheared pure cholesteric phase. Distortions of liquid crystalline order around water droplets may reduce the height of energy barrier for the creation of critical nuclei.

As the defects tend to fill all the available space through the second step ($t > 10\,\mathrm{s}$), the distribution of point defects becomes largely periodic. This indicates the existence of a repulsive interaction between point defects. When two point defects mutually approach, the elastic energy increases owing to the distortion of the liquid crystalline order induced by the mismatch of the cholesteric helix. This elastic interaction between point defects can be sufficiently large to drive the periodicity of the defect array.

## CONCLUSION

We found that the regular defect array is formed spontaneously after stopping the shear in the cholesteric emulsions for the first time. There are two steps in the formation process of the defect array. The first step is the nucleation and the growth of point defects from the planar texture. Water droplets play a role to reduce the barrier energy to make nuclei of point defects, by distorting the liquid crystalline order. On the contrary, the second step is the regular rearrangement to the defect array. When all space is filled up by defects, the regularity in the period of point defects appears owing to the interaction between neighboring defects, which is introduced by elastic spatial distortion of the cholesteric helix.

## REFERENCES

[1] Poulin, P., Stark, H., Lubensky, T. C., & Weitz, D. A. (1997). *Science*, *275*, 1770.
[2] Lev, B. I. & Tomchuk, P. M. (1999). *Phys. Rev. E*, *59*, 591.
[3] Poulin, P. & Weitz, D. A. (1998). *Phys. Rev. E*, *57*, 626.
[4] Lubensky, T. C., Petty, D., Currier, N., & Stark, H. (1998). *Phys. Rev. B*, *57*, 610.
[5] Monval, O. M., Dedieu, J. C., Krzywicki, T. G., & Poulin, P., (1999). *Eur. Phys. J. B.*, *12*, 167.
[6] Lanzo, J., Nicoletta, F. P., Filpo, G. D., & Chidichimo, G. (2000). *Liq. Cryst.*, *27*, 1029.
[7] Yamamoto, J. & Tanaka, H. (2001). *Nature*, *409*, 321.
[8] Bouligand, Y. (1972). *J. Phys.*, *33*, 715.
[9] Bates, F. S. & Wiltzius, P. (1989). *J. Chem. Phys.*, *91*, 3258.
[10] Tanaka, H. (1995). *Phys. Rev. E*, *51*, 1313.